JOURNAL OF MATERIALS SCIENCE **39** (2004) 1671 – 1675

RF sputtering deposition of $MgMn_2O_4$ spinel thin films

L. MALAVASI*
INSTM, IENI/CNR, Dipartimento di Chimica Fisica "M. Rolla", Università di Pavia,
Viale Taramelli 16, I-27100, Pavia, Italy
E-mail: malavasi@chifis.unipv.it

M. C. MOZZATI
INFM, Unità di Pavia and Dipartimento di Fisica "A. Volta", Università di Pavia, Via Bassi 6,
I-27100, Pavia, Italy

G. CHIODELLI
INSTM, IENI/CNR, Dipartimento di Chimica Fisica "M. Rolla", Università di Pavia,
Viale Taramelli 16, I-27100, Pavia, Italy

C. B. AZZONI
INFM, Unità di Pavia and Dipartimento di Fisica "A. Volta", Università di Pavia, Via Bassi 6,
I-27100, Pavia, Italy

G. FLOR
INSTM, IENI/CNR, Dipartimento di Chimica Fisica "M. Rolla", Università di Pavia,
Viale Taramelli 16, I-27100, Pavia, Italy

In this paper we describe about the synthesis of $MgMn_2O_4$ thin films by means of off-axis RF magnetron sputtering and their structural and morphological characterisation realised by means of X-ray diffraction (XRD), micro-Raman spectroscopy and Scanning Electron Microscopy (SEM). We explored different synthesis conditions, namely the substrate temperature, T_s, and the sputtering gas composition and we could observe that well-crystallised films are obtained at $T_s = 500°C$ while the effect of the sputtering gas composition is to affect the structural properties of the films deposited. The thin films deposited always present a crystal structure less distorted with respect to the one of the target material. The possibility of synthesising films of low distorted spinels or even cubic ones may be an interesting way of preparing buffering layers for the growth of isostructural materials such as other spinels or pseudocubic perovskites.

1. Introduction

Manganese spinel oxides of general formula AMn_2O_4 (A = Cd, Mg, Zn, Mn) are attractive materials due to their structural, chemical and physical properties. Some compounds of this class turned out to be promising materials for mixed potential devices for sensing oxygenic gases, such as NO_x [1–3]. Despite $CdMn_2O_4$ resulted to be the more suitable for sensitivity to NO_x, isostructural systems, such as $MgMn_2O_4$, could be preferred for their lower toxicity. Bulk $MgMn_2O_4$ is a tetragonal partially inverted spinel and it can also exist in the cubic form if a very high inversion degree is reached [4]. Indeed, in the direct spinel, only the Mn(III) oxidation state is expected for manganese (Jahn-Teller ion), while the partial inversion induces the formation of Mn(IV) and Mn(II) ions in octahedral and tetrahedral sites, respectively [5], so influencing the physical properties of this system.

Vast literature is devoted to the study of magnetic, transport and structural properties of $MgMn_2O_4$ bulk material [4–12]. Nevertheless this spinel synthesised as thin film may present attractive applicative possibility. For example, the coexistence of Mn(III) and Mn(IV) ions in the octahedral spinel sublattice, as consequence of the spinel inversion, favours the catalytic processes and so the employment of the material as sensor device, in analogy with other manganese-based oxides [13]. To our knowledge, no thin films preparation of this spinel oxide has been reported till now.

In this paper we describe about the synthesis of $MgMn_2O_4$ thin films by means of off-axis RF magnetron sputtering and their structural and

---

*Author to whom all correspondence should be addressed.

morphological characterisation realised by means of X-ray diffraction (XRD), micro-Raman spectroscopy and Scanning Electron Microscopy (SEM).

2. Experimental

Thin films of $MgMn_2O_4$ were grown starting from pressed powders of $MgMn_2O_4$ target material obtained by solid state reaction. Details about the target preparation and characterisation were reported previously [8].

In the thin films preparation we investigated the role of the atmosphere composition in the chamber and the substrate temperature T_s. The films were grown onto commercial Al_2O_3; substrates were rotated during deposition and the temperature T_s was measured by means of a thermocouple located immediately under the substrate. First we made the depositions employing as sputtering gas a mixture of argon/oxygen in the ratio 5:1, with a total pressure of 0.015 mbar, both with substrate heating ($T_s = 500°C$) and without substrate heating. The latter samples underwent thermal treatments after the deposition: they were annealed at two different temperatures ($T_{ann} = 400$ and $600°C$) in pure oxygen for 2 h. Other depositions were performed in pure argon with substrate heating at 500°C. The rate deposition at 100 W was around 2.5 nm/min when working with argon/oxygen and around 6 nm/min for pure argon. Thin films thickness, measured by means of a profilometer, was around 700 nm.

SEM measurements were performed with an Oxford Stereoscan. Film composition was measured by means of microprobe analysis and the chemical composition of the deposited films was found to be in fairly good agreement with the target composition for both gas mixtures.

X-ray diffraction patterns were acquired on a Philips 1710 diffractometer equipped with a Cu anticathode, adjustable divergence slit, graphite monochromator on the diffracted beam and proportional detector.

Micro-Raman measurements were carried out with a Labram Dilor Raman spectrometer, equipped with Olympus microscope HS BX40. The beam of a He-Ne laser at 632.8 nm was focussed on a surface of about 2 μm diameter.

3. Results and discussion

Fig. 1 reports the X-ray diffraction patterns, acquired at a fixed incident angle of 2°, for the $MgMn_2O_4$ films deposited in argon/oxygen together with the X-ray diffraction pattern of the target material. Pattern (a) refers to a film deposited without substrate heating while pattern (b) is relative to a film deposited by heating the substrate ($T_s = 500°C$). The vertical lines in the plot correspond to the reference diffraction peaks of the substrate [14]. In the presented patterns of the films only one clearly detectable peak can be found at about 19°. The full width at half maximum (FWHM) for this peak is 1.16° for sample (a) and 0.455° for sample (b). As can be inferred, the film deposited without substrate heating is poorly crystallised if compared with the one deposited under substrate heating.

The crystallinity of the film deposited without substrate heating is improved by the annealing treatments.

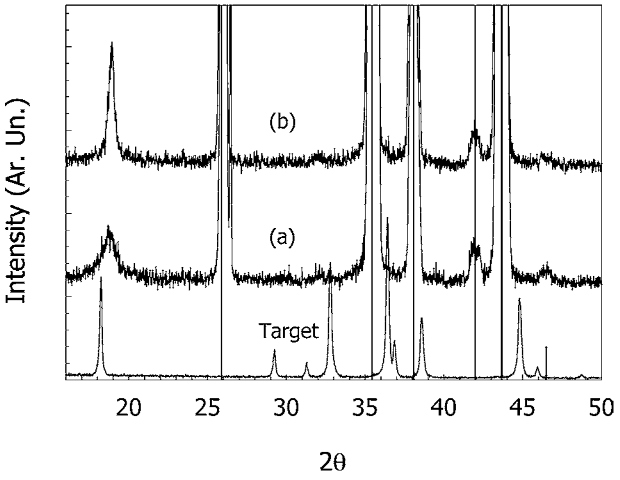

Figure 1 X-ray pattern of as-deposited $MgMn_2O_4$ thin films without (a) and with (b) substrate heating in argon/oxygen environment. For comparison the X-ray diffraction pattern of the target material is also displayed. The vertical lines correspond to the Al_2O_3 reference diffraction peaks.

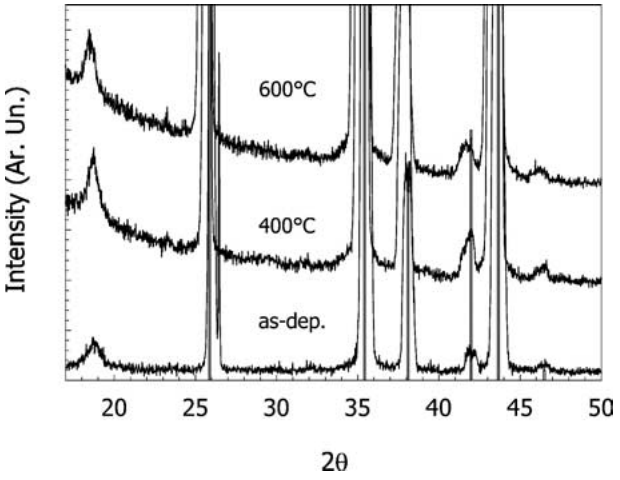

Figure 2 X-ray pattern of as-deposited $MgMn_2O_4$ thin films (as-dep.) and after a thermal treatment at 400°C (400°C) and 600°C (600°C). The vertical lines correspond to the Al_2O_3 reference diffraction peaks.

This is evident from Fig. 2, where the X-ray pattern of the as-deposited film is displayed together with those collected after the annealing at 400°C and at 600°C: the visible diffraction peak is narrower for the annealed samples. Anyway, also in these cases the only clearly visible peak is the one located at about 19°.

Depositions of $MgMn_2O_4$ films in pure Argon with $T_s = 500°C$ have been successively performed to check the possibility to further improve the film crystallinity. Fig. 3 presents the X-ray diffraction characterisation for these films together with the pattern of the target material. For comparison, the reference lines of a pertinent cubic phase (black lines) are also reported: since no tabulated JCPDS card for the cubic $MgMn_2O_4$ spinel is available we used, as reference, the one of the cubic Mn_3O_4 [15], which just exhibits a tetragonal to cubic structural transition at about 1160°C and is isostructural to $MgMn_2O_4$. A nice correspondence can be observed between the diffraction peaks of the films and those related to the cubic phase of Mn_3O_4, taking into account that a slightly different peak position can be ascribed to a different lattice parameter. The grey solid reference lines are instead related to the substrate peaks.

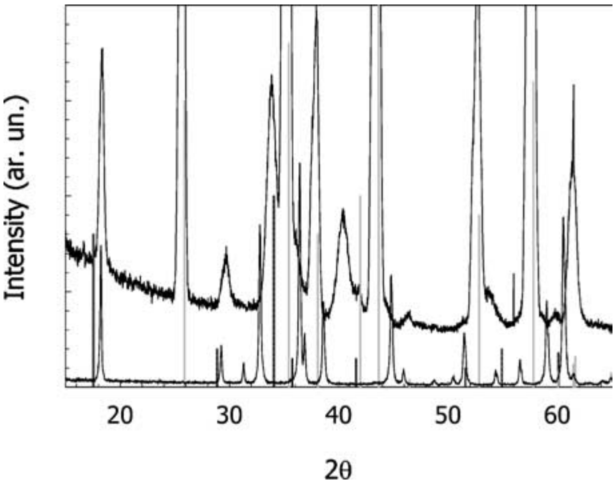

Figure 3 X-ray pattern of as-deposited $MgMn_2O_4$ thin films with substrate heating in pure argon. For comparison the X-ray diffraction pattern of the target material is also displayed. The grey solid lines refer to the substrate peaks while the black ones refer to the cubic phase of Mn_3O_4.

The different X-ray behaviours observed for the two series of films cannot be ascribed to differences in the chemical composition, due to the results of the microprobe analysis. As regards the patterns of the film deposited under argon/oxygen, the evidence of only one diffraction peak makes the definition of the crystal structure difficult. Indeed for both tetragonal and cubic structures a diffraction peak is found around 19° corresponding to the (101) reflection for the tetragonal structure and to the (111) for the cubic one. For the tetragonal structure and when the material is direct this peak is particularly intense while for the cubic one the (111) reflection constitutes one of the most intense peak for each cation distribution. So the only plausible information from the X-ray diffraction characteristics for the films deposited under argon/oxygen may be a preferential growth along one crystallographic direction, that is the (100) or the (111) one, depending on the crystal structure. At this stage is therefore not possible to say anything conclusive about the crystal structure of the material from XRD results. For the films deposited in pure argon environment the correspondence of the diffraction peaks with those related to the cubic spinel phase points out the formation of this phase with a random grains orientation.

The formation of the $MgMn_2O_4$ cubic phase is possible if the material displays a relevant inversion degree, i.e., many Mg(II) ions are placed in the octahedral sites. Indeed the $MgMn_2O_4$ spinel has a tetragonal crystal structure (space group $I4_1/amd$) when the cation arrangement is normal, i.e., all the magnesium ions are placed on the A sites and all the manganese ions on the B sites, or in the case of relatively low inversion degree (<30–35%). On the contrary when it is highly inverted its crystal structure is cubic (space group $Fd3m$) [10, 11]. In the present case, as can be also inferred from the X-ray patterns of Figs 1 and 3, the $MgMn_2O_4$ used as target material for the deposition possess a tetragonal structure. This agrees with the typical behaviour of bulk material: when slowly cooled to room temperature it shows a relatively low inversion degree, this value being evaluated between 2% [9] and 20% [8]. The inversion degree increases starting from about 600°C but a relevant inversion, such to generate a cubic phase, is achievable only for $T > 1000°C$ [10, 11].

So, the deposition temperature used for our films (500°C) is not high enough to allow the development of an equilibrium distribution of the cations between the A and B sites of the spinel in order to give rise to the cubic structure. Rather, the presence of such a phase may arise from the random distribution of the magnesium and manganese cations in the spinel octahedral and tetrahedral sites, also taking into account that a complete miscibility exists in the $MgMn_2O_4$-Mn_3O_4 solid solution [8, 9].

Some more insight about the structural properties and the nature of the deposited films can be obtained by means of micro-Raman spectroscopy. This technique also allows checking the homogeneity of the deposited material: in our case, the very high reproducibility of the Raman spectra on the whole surface of the considered films indicated a good homogeneity of the samples.

In the past we already analysed the Raman features of tetragonal manganese-based spinel bulk materials. In particular we considered the relationship between cation distribution and Jahn-Teller phonons. Besides, we studied the inversion degree of slowly cooled $MgMn_2O_4$ samples by analysing the Raman spectra of both the $MgMn_2O_4$-Mn_3O_4 solid solution and of $MgMn_2O_4$ samples quenched from high different temperatures thus characterised by a very high inversion degree and a nearly cubic structure [16]. On the basis of these results we now analyse the Raman spectra collected for the $MgMn_2O_4$ thin films.

Fig. 4 shows some selected spectra for the as-deposited films together with the Raman spectra of the target material and of the substrate. Fig. 4a refers to a film deposited at $T_s = 500°C$ in argon/oxygen environment while Fig. 4b refers to a sample prepared at $T_s = 500°C$ with only argon in the chamber. In both cases the presence of the substrate signal is evident and this partly reduces number and quality of the information we can deduce from these measurements. For the spectra of the film in Fig. 4a, a peak near 700 cm^{-1} is evident beside the Al_2O_3 signal. This can be assessed due to the different relative intensity of the Al_2O_3 peaks. A less evident feature is present around 500 cm^{-1}. No other structure is detectable in these spectra. In the Raman spectra of the other sample (Fig. 4b) the presence of two structures at about 580 and 670 cm^{-1} can be noticed. Another broad and low-intensity feature is found around 340 cm^{-1}.

The results of the Raman characterisation point out that the spectra of both films differ from that of the tetragonal target material. The presence of a reduced number of Raman peaks is a clear evidence of a higher symmetry of the deposited material with respect to the target. In the Raman spectra of both films we can find the main features usually recorded in cubic spinels belonging to the $Fd3m$ space group [16–18], even if there is a quite high spread in the features of the published

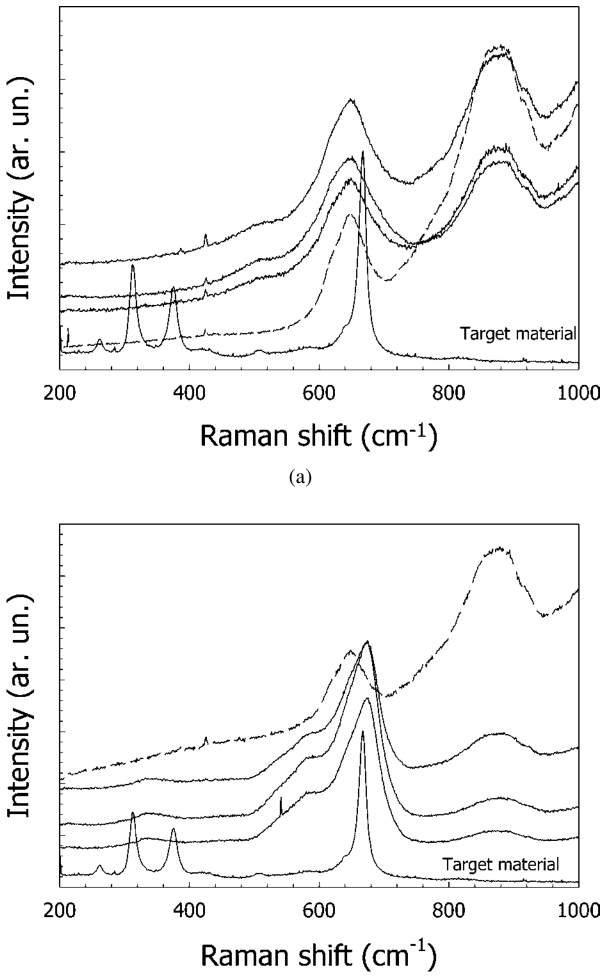

(a)

(b)

Figure 4 Raman spectra of $MgMn_2O_4$ this films deposited in argon/oxygen (a) and pure argon (b). For comparison the spectra of the target material and of the substrate (dashed lines) are also displayed.

spectra for the cubic spinels, since they are deeply affected by many variables such as the firing temperature or the gas environment used in the thermal processes. Nevertheless, by comparing the Raman spectra of the considered $MgMn_2O_4$ films with those of our $MgMn_2O_4$ powder samples quenched from high temperature (and so highly inverted) [16], a noticeable correspondence can be observed when the films are grown in pure argon atmosphere. For the film deposited in argon/oxygen environment, the lower number of peaks in the spectra could also be a consequence of a higher symmetry related to a preferential growth along one crystallographic direction, as previously suggested by the XRD results.

Scanning electron microscopy characterisation is displayed in Fig. 5 at 3 000× and 10 000× for the two films: Fig. 5a refers to the material deposited in argon/oxygen while 5b is relative to a sample deposited with pure argon. From the low enlargement images it is possible to note a similar morphology for both materials: they are constituted of grains of few microns. At higher enlargement the morphology of the two films appears different. In particular it is possible to appreciate that the films prepared in an argon/oxygen environment display a microstructure in which a lamellar morphology is recognisable while this feature is not encountered for the other series of film. This seems to agree with the X-ray diffraction and micro-Raman results which suggest an iso-oriented growth for the film deposited in argon/oxygen. Anyway, a more detailed study about the morphology of the two different films and in particular the deepening of the hypothesed lamellar growth for the film deposited in argon will be matter of future work since it goes beyond the scope of the present work.

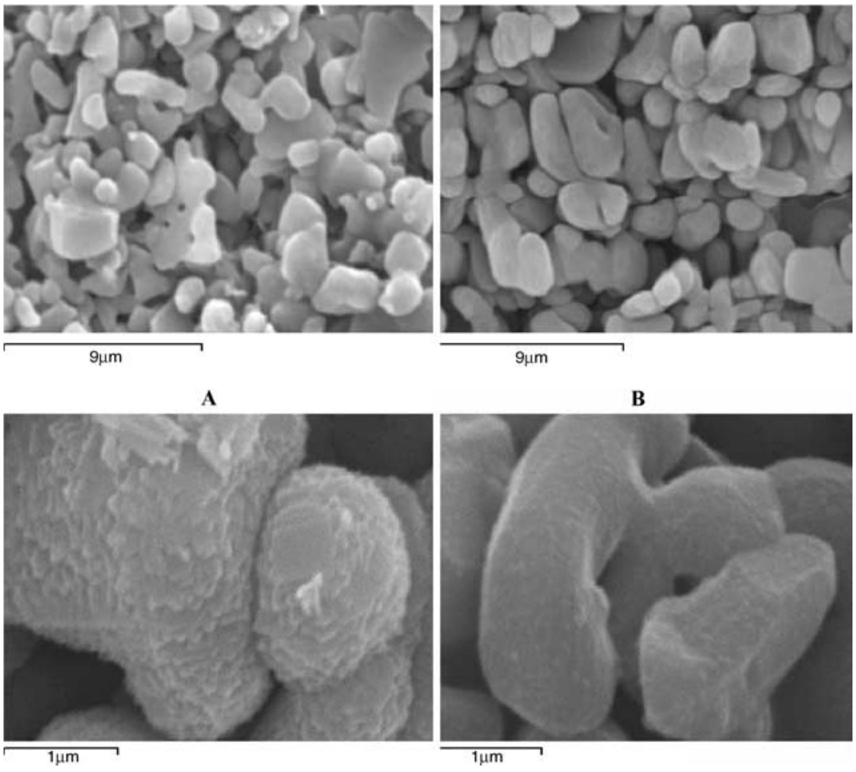

Figure 5 SEM images of $MgMn_2O_4$ thin films deposited in argon/oxygen (a) and in pure argon (b) at 3 000× (upper part) and 10 000× (at the bottom).

4. Conclusion

In this work we performed the deposition of $MgMn_2O_4$ spinel thin films by means of RF-sputtering, exploring different synthesis conditions, namely the substrate temperature, T_s, and the sputtering gas composition. Well-crystallised films are obtained at $T_s = 500°C$. The deposition rate increases when working in pure argon with respect to the deposition in an argon/oxygen environment and this might be related to the different morphology of the films: X-ray diffraction suggests a preferential growth when working at the lowest deposition rate. This has been also supported by the SEM inspection and is consistent with micro-Raman results.

Micro-Raman and X-ray diffraction information points out that the grown films are not highly distorted tetragonal spinels like the target material but display a less distorted structure, possibly the cubic one. As a consequence, highly inverted spinels are formed also at low temperature, with the removal of Mn(III) Jahn-Teller ions from the octahedral sites [6, 9, 10] and the formation of Mn(IV) ions in the same sites. This is important for the employment of these materials as sensor devices because the coexistence of Mn(III) and Mn(IV) ions favours the catalytic processes. Moreover, we remark that in the usual synthetic conditions adopted for the preparation of $MgMn_2O_4$ powders it is not easy to achieve a pure cubic phase as a consequence of the high temperature required for a high inversion to occur. The possibility of synthesising films of low distorted spinels or even cubic ones may be an interesting way of preparing buffering layers for the growth of isostructural materials such as other spinels or pseudocubic pervoskites.

Acknowledgments

This work has been partially supported by Progetto Finalizzato MSTA II.

The Laboratory of "Chimica Strutturistica" of University of Brescia is gratefully acknowledged for having performed EMPA analysis. S. Aldrovandi is acknowledged for technical support.

Dr. Eliana Quartarone is gratefully acknowledged for assistance during films deposition.

References

1. N. YAMAZOE and N. MIURA, *Solid State Ionics* **86–88** (1996) 987.
2. N. MIURA, G. LU and N. YAMAZOE, *J. Electrochem. Soc.* **143** (1996) 2.
3. N. MIURA, H. KUROSAWA, H. HASEI, G. LU and N. YAMAZOE, *Solid State Ionics* **86–88** (1996) 1069.
4. F. DRIESSENS, *Inorg. Chem. Acta* **1** (1967) 193.
5. M. ROSEMBERG and P. NICOLAU, *Phys. Stat. Sol.* **6** (1964) 101.
6. P. GHIGNA, G. FLOR and G. SPINOLO, *J. Solid State Chem.* **149** (2000) 252.
7. P. GHIGNA, G. B. BARBI, G. CHIODELLI, G. SPINOLO, L. MALAVASI and G. FLOR, *ibid.* **153** (2000) 231.
8. L. MALAVASI, P. GHIGNA, G. CHIODELLI, G. MAGGI and G. FLOR, *ibid.* **166** (2002) 171.
9. C. B. AZZONI, M. C. MOZZATI, L. MALAVASI, P. GHIGNA and G. FLOR, *Solid State Commun.* **119** (2001) 591.
10. C. B. AZZONI, M. C. MOZZATI, P. GHIGNA, L. MALAVASI and G. FLOR, *ibid.* **117** (2001) 511.
11. R. MANAILA and P. PAUSESCU, *Phys. Stat. Sol.* **9** (1965) 385.
12. N. K. RADHAKRISHNAN and A. B. BISWAS, *ibid.* **37** (1976) 719.
13. L. A. PEDERSEN and W. F. LIBBY, *Science* **176** (1972) 1355.
14. Card number 71-1683.
15. Card number 13-0161.
16. L. MALAVASI, P. GALINETTO, M. C. MOZZATI, C. B. AZZONI and G. FLOR, *Phys. Chem. Chem. Phys.* **15**(4) (2002) 3876.
17. B. AMMUNDSEN, G. R. BURNS, M. S. ISLAM, H. KANOH and J. ROZIÈRE, *J. Phys. Chem.* B. **103** (1999) 5175.
18. S. R. S. PRABAHARAN, N. B. SAPARIL, S. S. MICHAEL, M. MASSOT and C. JULIEN, *Solid State Ionics* **112** (1998) 25.

Received 24 March
and accepted 21 October 2003